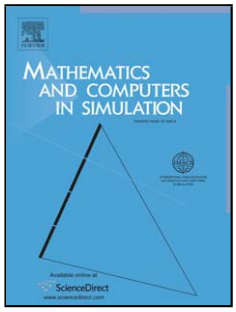

Title: An overlapping mortar element approach to coupled magneto-mechanical problems

Author: Francesca Rapetti

PII: S0378-4754(09)00046-9
DOI: doi:10.1016/j.matcom.2009.02.008
Reference: MATCOM 3185

To appear in: *Mathematics and Computers in Simulation*

Received date: 6-11-2008
Revised date: 22-1-2009
Accepted date: 16-2-2009

Please cite this article as: F. Rapetti, An overlapping mortar element approach to coupled magneto-mechanical problems, *Mathematics and Computers in Simulation* (2008), doi:10.1016/j.matcom.2009.02.008

An overlapping mortar element approach to coupled magneto-mechanical problems

Francesca Rapetti

Lab. J.-A. Dieudonné, CNRS & Université de Nice Sophia-Antipolis, Parc Valrose, 06108 Nice cedex 02, France

Abstract

This paper presents a finite element approach with moving non-matching overlapping grids to solve coupled magneto-mechanical problems. As an example of application, we consider the team workshop problem 28 for an electrodynamic levitation device. The connection between the background mesh including the two exciting coils and the foreground mesh of the conducting plate is established by using a stable projection operator onto the plate boundary. The aim is to determine the dynamic characteristics of the levitating plate: to this end, a coupled solution of the electromagnetic and mechanical problem is necessary.

Key words: nested domains, mortar finite elements, axisymmetric geometries
PACS: 35Q60, 65N30, 65M55, 68U20

1 Introduction

Electromagnetic devices which convert electrical energy into useful and controllable mechanical work are used in many engineering areas. Examples of these devices include electric motors, circuit breakers, actuators, etc. The discretization of these devices containing moving part is not an easy task when dealing with finite elements. Even small displacements cause a distortion of the mesh, leading to a reduction of the mesh quality (presence of stretched or irregular elements) as well as of the solution accuracy. Large displacements require frequent remeshing of the whole device, due to the continuously changing position of the moving parts. The unknowns on the new mesh have to be related to the unknowns on the old mesh, causing light perturbations on the final solution. This disadvantage can be overtaken by considering suitable techniques.

In this paper we consider an variational non-conforming domain decomposition approach which allows to work with non matching grids in different parts of the device. The difficulty relies on finding suitable projection operators between the involved meshes. Standard Lagrange interpolation operators are not enough accurate due to insufficient stability properties. Mortar finite element techniques, firstly proposed in [3] for nonoverlapping subdomains, yield optimal a priori error estimate also in the case of overlapping subdomains, see [1,6] and the references therein. They allows an efficient coupling of different physical models, discretization schemes or non-matching triangulations in the subdomains. The main feature of the mortar element method is to replace the exact continuity condition at the skeleton of the decomposition with a weak one, that can be written in terms of a Lagrange multiplier and the jump of the traces. Quadrature formulas are used to evaluate the associated integrals, involving discrete functions defined on different non-matching grids. Due to its high flexibility, this approach has been analysed and implemented in many situations. Alternative techniques to handle nested domains are provided by the so-called Chimera methods [5], fictious domain methods [9], the finite element method with patches [10], the FEM-BEM coupling [12].

This work is devoted to an *overlapping* version of mortar element method different from the one proposed in [1,6] and its application (in two dimensions) to compute eddy currents in a moving conductor (see [2,4] for different formulations and finite element discretizations of the eddy-current problem). The overlapping feature is appreciated in absence of interfaces which are invariant with respect to the movement, *e.g.*, with conductors freely moving in a magnetic field. Both the global domain and the moving subdomain are discretized by completely independent meshes, each of which following the movement of the related subdomain during the computation. No remeshing is then necessary. The data transmission between the two meshes is managed by a projection operator onto the subdomain boundary which has to satisfy some stability and approximation requirements. Only the matrix representing the projection operator has to be reassembled as soon as the subdomain position changes. We focus on the method application to coupled magneto-mechanical problem with a rotational symmetry. To this end, we adopt a one-directional coupling (the solution on the global domain defines the boundary data for the problem on the subdomain) which is a derivation of a more complex two-directional one presented in [7] to numerically simulate an electromagnetic braking system. The same one-directional coupling is applied in [8] to elasticity and analysed in the case where different meshwidths and polynomial orders are used on the subdomains.

After the presentation of the continuous problem in Section 2, the discrete one is formulated in Section 3. The corresponding algebraic system and implementation details are presented in Section 4 whereas Section 5 is dedicated to numerical results, including the application to the levitation problem [11].

2 The model

We consider an electrodynamic levitation device consisting of a conducting plate over two exciting coils, all of them with an axial symmetry (Fig. 1 left). It will be assumed that there are neither displacement currents nor surface currents, and that the inductors are supplied with a sinusoidal current having a prescribed intensity. We neglect for simplicity the eddy current reaction field to the exciting coils. Further developments to consider a levitation plate with an eccentric bore which disturbs the axisymmetry and requires a full 3D modeling as well as different geometries and operating frequencies in presence of voltage driven exciting coils would be interesting to do but beyond the scope of the present work.

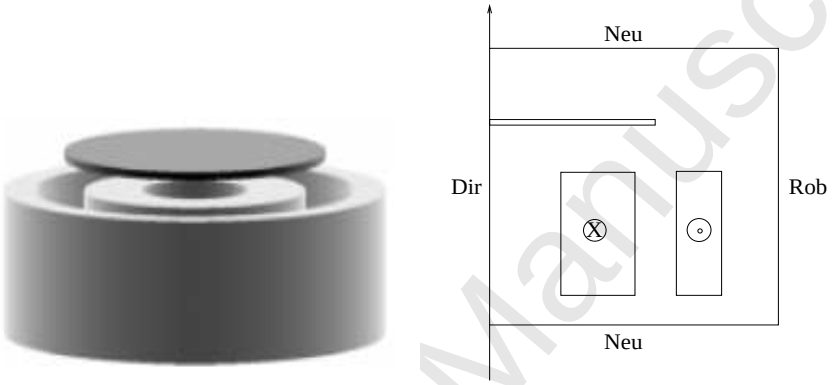

Fig. 1. Electrodynamic levitation device and computational domain cross section with boundary conditions.

The mathematical model describing the eddy current problem in the plate at low frequency is given by the quasi-stationary Maxwell equations [2]. In this paper we are interested in the magnetic field computation and the magnetic vector potential is chosen as primary variable to describe the physical phenomena.

The space $\mathbb{R}^3$ is decomposed into the conducting region V_c and the external region $\mathbb{R}^3 \setminus V_c$. Denoting by H, B, J and E the magnetic field, the magnetic flux density, the current density and the electric field, respectively, the quasi-stationary Maxwell's equations in V_c and $V \setminus V_c$ read

$$\nabla \times H = J\mathcal{I}_{V_c} + J_s\mathcal{I}_{V\setminus V_c}, \quad \nabla \times E = -\partial_t B, \quad \nabla \cdot B = 0 \tag{1}$$

where ∂_t denotes the first order partial derivative with respect to the time variable t and $\mathcal{I}_D(\mathbf{x}) = 1$ if $\mathbf{x} \in D$ otherwise 0. The densities and the fields are linked by the constitutive properties, *i.e.*, $B = \mu H$, $J = \sigma E$, where $\mu > 0$ is the magnetic permeability and $\sigma \geq 0$ stands for the electric conductivity. Moreover, we assume that the material parameters are time independent and

associated with linear isotropic media, and that the given external source J_s is zero within the conducting region V_c. The problem is well posed by adding regularity conditions at infinity, and suitable interface conditions on ∂V_c. In particular, $[H]_c \times n_c = 0$, $[B]_c \cdot n_c = 0$, together with $[E]_c \times n_c = 0$, $[J]_c \cdot n_c = 0$, where n_c is the outer normal on ∂V_c and $[v]_c$ stands for the jump of v on ∂V_c. Additionally to the boundary conditions, we have to impose suitable initial values for the vector fields at a given time t_0. The initial condition on B has to satisfy $\nabla \cdot B = 0$ and $[B] \cdot n = 0$ at any interface. We can work on a bounded domain V by introducing artificial boundary conditions. For simplicity, we assume that V_c is a simply connected polyhedral subdomain of V and that $\overline{V_c} \subset V$.

We now take advantage of the problem geometry axial symmetry. Let (e_r, e_θ, e_z) be the natural tangent system associated with the cylindrical coordinates (r, θ, z) such that the Oz-axis is the symmetry axis of the levitation device. The current density J is supposed to be of the form $J = \mathcal{J}(r, z, t)e_\theta$, and so for the source current J_s. It is also assumed that the components of the fields H, E, B in the system (e_r, e_θ, e_z) depend only on r, z and t (not on θ). Ampere's theorem yields then a magnetic field H of the form $H = H_r(r, z, t)e_r + H_z(r, z, t)e_z$. For the magnetic density B, the condition $\nabla \cdot B = 0$ suggests the introduction of a (magnetic) vector potential A such that $B = \nabla \times A$. Maxwell's equations in terms of the magnetic vector potential A become:

$$\nabla \times (\nu \nabla \times A) + \sigma \partial_t(A)\, \mathcal{I}_{V_c} = J_s\, \mathcal{I}_{V \setminus V_c} \tag{2}$$

where $\nu = \frac{1}{\mu}$. We take A of the form $A = \mathcal{A}(r, z, t)e_\theta$, in such a way that A is divergence-free (Coulomb gauge). Note that $\nabla \times A = (1/r)\nabla(r\mathcal{A}) \times e_\theta$. Using the notation $B = B_r(r, z, t)e_r + B_z(r, z, t)e_z$, we get $B_r = -\partial_z \mathcal{A}$ and $B_z = (1/r)\partial_r(r\mathcal{A})$. Thanks to the axial symmetry, equation (2) reads:

$$-\partial_r\left(\frac{\nu}{r}\partial_r(r\mathcal{A})\right) - \partial_z\left(\nu \partial_z(\mathcal{A})\right) + \sigma \partial_t(\mathcal{A})\, \mathcal{I}_{V_c} = J_s\, \mathcal{I}_{V \setminus V_c} \tag{3}$$

For the numerical computations, we shall consider a rectangular box $\Omega = [0, R] \times [z_1, z_2] \subset V$ in the (r, z)-plan, with R, z_1 and z_2 big enough for the magnetic field to be weak at the boundary of the box and set $\Omega_c = \Omega \cap V_c$. The Biot-Savart hypothesis implies that the field B behaves like $1/(r^3 + z^3)$ far from the conductors. For big values of r, the behavior of $\mathcal{A}$ can be assumed similar to $1/r^2$. Therefore, on the boundaries Γ_R of Ω which are parallel to the symmetry axis (here $\Gamma_R = \{(R, z),\ z_1 \leq z \leq z_2\}$) we impose a so-called Robin condition $\partial_r(r\mathcal{A}) + \mathcal{A} = 0$. For those boundaries of Ω which are perpendicular to the symmetry axis, a Robin-like condition is difficult to enforce. Instead, we set the Neumann condition $\partial_z(r\mathcal{A}) = 0$ which stems from the assumption that the radial component of the magnetic field is close to zero on these boundaries. Finally, the natural symmetry condition along the symmetry axis is a Dirichlet

one, *i.e.*, $\mathcal{A} = 0$ (Fig. 1 right). The two interface conditions on ∂V_c read respectively $[\mathcal{A}]_c = 0$ the first, and $[\partial_r(r\mathcal{A})]_c = 0$ on the vertical parts of ∂V_c which are parallel to the symmetry axis or $[\partial_z \mathcal{A}]_c = 0$ on the horizontal parts of ∂V_c which are perpendicular to the symmetry axis, the second.

For the mechanical equations, only rigid body motions are considered. We denote by m the mass of Ω_c. The levitation height z refers to the distance between the lowest edge of the plate Ω_c and the uppest edge of the current carrying area ($z = 0$), with initial conditions on position $z(0)$ and velocity $v(0)$. Neglecting any movement parallel to the (r, θ)-plane, the Newton's law of motion for the point mass $(0, 0, z)$ reads:

$$m\dot{v} = F, \qquad \dot{z} = v, \tag{4}$$

where the total external force F includes the gravity force pulling downward and the external magnetic force $(F_m)_z = (\int_{\Omega_c} J \times B)_z$. In axisymmetric configurations, we have $(F_m)_z = -2\,\pi \int_{\Omega_c} \sigma\, \partial_t(\mathcal{A})\, B_r\, r\, dr\, dz$.

Remark. Electrodynamic levitation is based on the induction of eddy currents in conducting materials. These eddy currents can be induced in non-moving conductors by a time varying magnetic field, or by constant magnetic fields in moving conductors, or a combination of the two configurations. In the considered configuration, the conductor Ω_c can freely move in Ω. In presence of moving conductors, we have to choose the reference system with respect to which we write the eddy current problem. Let $\mathcal{R}$ be a reference system linked to Ω and $\mathcal{R}_c$ be a reference system linked to Ω_c. If v is the conductor velocity, the appropriate form of Ohm's law linking the (induced) current J to the electric field E in the reference system $\mathcal{R}$ reads

$$J = \sigma(E + v \times B) \qquad \text{in } \Omega_c \qquad \text{and} \qquad J = \sigma\, E \qquad \text{in } \Omega.$$

The motion of Ω_c is directly considered in the convective term $v \times B$. This is a typical feature of the Eulerian description, *i.e.* the use of a single reference system $\mathcal{R}$ for both parts Ω and Ω_c. To get rid of the explicit velocity term, it is advisable to use as many different frames as the number of parts, that is, in our case, to reformulate with respect to $\mathcal{R}$ the equations in Ω and with respect to $\mathcal{R}_c$ the equations in Ω_c. This is the Lagrangian description, where the spectator is attached to the considered part and describes the events from his material point of view. This approach makes disappear the explicit velocity term from Ohm's law, provided that each part is treated in its own "co-moving" frame ($\mathcal{R}$ always still in Ω and $\mathcal{R}_c$ co-moving with Ω_c). It remains to couple at the conductor boundary the computations lead in the two parts by means of transmission conditions, which will be weakly imposed in the considered overlapping finite element approach. We stress the fact that for the analysis

of eddy current problems in domains with moving parts, there is freedom in the choice of the reference frame, provided that the conductor velocity can be regarded as non-relativistic, which is the case here. This is a consequence of the low frequency limit and not valid for the full set of Maxwell's equations. Thanks to this characteristic of the eddy current model, we can adopt the "piece-wise Lagrangian approach" (a Lagrangian approach on each part). This allows to work with independent meshes and discretization basis, as we are going to describe in what follows.

3 Discretization

We adopt a non-conforming overlapping mortar element approach coupled with standard $\mathbb{P}_1$ finite elements in Ω and Ω_c and first order implicit finite differences in time for the discretization of equation (3).

We first solve problem (3) in Ω, and consecutively an additional problem in Ω_c, taking as Dirichlet data the restriction of the solution of (3) to the interface $\Gamma := \partial\Omega_c$. We restrict ourselves to the system obtained after time discretization of (3) by a stable implicit Euler scheme with time step δt. At each time step, we solve the following variational problems in Ω and Ω_c. Find $(\mathcal{A}, \mathcal{A}_c) \in H^1_{0,D}(\Omega) \times H^1_{\mathcal{A},\Gamma}(\Omega_c)$ such that

$$\begin{aligned} &\int_\Omega \tfrac{\nu}{r^2}\left(\partial_r(r\mathcal{A})\partial_r(r\phi) + \partial_z(r\mathcal{A})\partial_z(r\phi)\right) r\,dr\,dz \\ &\quad + \int_{\Gamma_R} \tfrac{\nu}{r}\phi\,\mathcal{A}\,r\,d\gamma = \int_{\Omega\setminus\Omega_c} \mathcal{J}_s\,\phi\,r\,dr\,dz, \qquad \forall \phi \in H^1_{0,D}(\Omega) \end{aligned} \tag{5}$$

and

$$\begin{aligned} &\int_{\Omega_c} \tfrac{\nu}{r^2}\left(\partial_r(r\mathcal{A}_c)\partial_r(r\phi_c) + \partial_z(r\mathcal{A}_c)\partial_z(r\phi_c)\right) r\,dr\,dz \\ &\quad + \int_{\Omega_c} \tfrac{\sigma}{\delta t}\phi_c\,\mathcal{A}_c r\,dr\,dz = \int_{\Omega_c} \tfrac{\sigma}{\delta t}\phi_c\,\tilde{\mathcal{A}}_c\,r\,dr\,dz, \qquad \forall \phi_c \in H^1_0(\Omega_c). \end{aligned} \tag{6}$$

where $H^1_{0,D}(\Omega) = \{v \in H^1(\Omega); v = 0 \text{ on the revolution axis}\}$, $H^1_{\mathcal{A},\Gamma}(\Omega_c) = \{v \in H^1(\Omega_c); v = \mathcal{A} \text{ on } \Gamma\}$, the unknowns $\mathcal{A}$ and $\mathcal{A}_c$ denote the approximations at the current time and $\tilde{\mathcal{A}}_c$ is the approximation of $\mathcal{A}_c$ at the previous time. Note that only the first transmission condition $[\mathcal{A}]_c = 0$ is explicitely enforced in $H^1_{\mathcal{A},\Gamma}(\Omega_c)$, the second condition $[\partial_r(r\mathcal{A})]_c = 0$ or $[\partial_z\mathcal{A}]_c = 0$ is embedded in the variational formulation and can be recovered by integration by parts. As we are going to describe later, at the discrete level the situation becomes more involved: the first transmission condition will be weakly imposed by means of a Lagrange multiplier space whereas the second condition is no more included in the variational formulation. The problem will not be solved

in the whole domain Ω but separately in $\Omega \setminus \Omega_c$ and Ω_c as the only matching (weakly) imposed on Γ is that of $\mathcal{A}$ and not that of $\partial_r(r\mathcal{A})$ on the vertical parts of Γ and that of $\partial_z\mathcal{A}$ on the horizontal parts of Γ.

A change in variables $u = r\mathcal{A}$ and $\psi = r\phi$ is employed to simplify the equations (5)-(6) as follows: find $(u, u_c) \in H^1_{0,D}(\Omega) \times H^1_{u,\Gamma}(\Omega_c)$ s. t.

$$\begin{aligned} &\int_\Omega \tfrac{\nu}{r}\left(\partial_r(u)\partial_r(\psi) + \partial_z(u)\partial_z(\psi)\right)\, dr\, dz \\ &\quad + \int_{\Gamma_R} \tfrac{\nu}{r^2}\psi\, u\, d\gamma = \int_{\Omega\setminus\Omega_c} \mathcal{J}_s\, \psi\, dr\, dz, \qquad \forall \psi \in H^1_{0,D}(\Omega) \end{aligned} \tag{7}$$

and

$$\begin{aligned} &\int_{\Omega_c} \tfrac{\nu}{r}\left(\partial_r(u_c)\partial_r(\psi_c) + \partial_z(u_c)\partial_z(\psi_c)\right)\, dr\, dz \\ &\quad + \int_{\Omega_c} \tfrac{\sigma}{r\,\delta t}\psi_c\, u_c\, dr\, dz = \int_{\Omega_c} \tfrac{\sigma}{r\,\delta t}\psi_c\, \tilde{u}_c\, dr\, dz, \qquad \forall \psi_c \in H^1_0(\Omega_c). \end{aligned} \tag{8}$$

It can be shown that problem (7)-(8) admits a unique solution thank to the Lax-Milgram lemma. In the continuous setting problem (7)-(8) at each time step yields the interface condition $u_c = u_{|\Omega_c}$, but at the discretization level, the situation becomes complex.

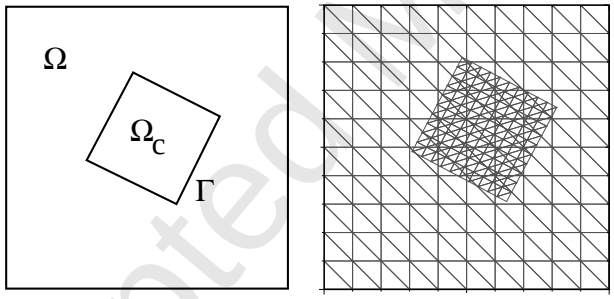

Fig. 2. Example of computational domain and overlapping meshes.

We use two different shape regular triangulations $\mathcal{T}_h$ on Ω and $\mathcal{T}_{h_c}$ on Ω_c, with h and h_c indicating the maximum element diameters, respectively. These overlapping triangulations are completely independent to each other, hence, in general, they do not match on Ω_c and the edges and faces of the triangulation $\mathcal{T}_{h_c}$ on the interface Γ also do not coincide with edges and faces of $\mathcal{T}_h$ (see Fig. 2 right). We use standard conforming finite elements of first order on $\mathcal{T}_h$ and $\mathcal{T}_{h_c}$, respectively. The associated discrete spaces with no boundary conditions are denoted by $X_h(\Omega)$ and $X_{h_c}(\Omega_c)$, respectively, and we set $X_{0,h}(\Omega) = X_h(\Omega) \cap H^1_0(\Omega)$ and $X_{0,h_c}(\Omega_c) = X_{h_c}(\Omega_c) \cap H^1_0(\Omega_c)$ to be the spaces taking into account homogeneous Dirichlet conditions on the revolution axis and Γ respectively. The trace space of $X_{h_c}(\Omega_c)$ on Γ is indicated by $W_{h_c}(\Gamma)$. We note that the restriction of a function $\psi \in X_h(\Omega)$ onto the interface Γ is, in general, not an element of $W_{h_c}(\Gamma)$. Thus, the Dirichlet problem on $X_{h_c}(\Omega_c)$ cannot be solved

directly, and a suitable operator $\Pi : X_h(\Omega) \to W_{h_c}(\Gamma)$ is required. In order to get optimal a priori error estimate (such that the global discretization error is bounded by the sum of the local ones times a constant that does not depend on the discretization parameters but on the solution), the operator Π has to be chosen as a projection on $W_{h_c}(\Gamma)$, *i.e.*, $\Pi v = v$ for all $v \in W_{h_c}(\Gamma)$, verifying

$$||\Pi v||_{\frac{1}{2},\Gamma} \leq C||v||_{\frac{1}{2},\Gamma}, \qquad \forall\, v \in H^1(\Omega),$$

with a constant C not depending on the meshsize h and where $||\cdot||_{\frac{1}{2},\Gamma}$ is the usual norm in $H^{\frac{1}{2}}(\Gamma)$. Thank to this assumption, the projection operator Π satisfies an approximation property of $H^{\frac{1}{2}}(\Gamma)$, namely, $||v-\Pi v||_{\frac{1}{2},\Gamma} \leq Ch|v|_{\frac{3}{2},\Gamma}$, for all $v \in H^1(\Omega)$. This projection operator plays an important role within the framework of mortar finite elements, as we will point out in the next section. We are now able to formulate the discrete variational problem: find $(u_h, u_{h_c}) \in X_{0,h}(\Omega) \times X_{u_h,h_c}(\Omega_c)$ s. t. equations (7)-(8) are verified for all functions $\psi_h \in X_{0,h}(\Omega)$ and $\psi_{h_c} \in X_{0,h_c}(\Omega_c)$, respectively, with $X_{u_h,h_c}(\Omega_c) := \{v \in X_{h_c}(\Omega_c) : v_{|\Gamma} = \Pi u_h\}$. The finite element solution u^* at each time is defined by u_h in $\Omega \setminus \Omega_c$ and u_{h_c} in Ω_c. Note that in general $u^* \notin H^1_0(\Omega)$. The error $u - u^*$ measured in the broken H^1-norm $||\cdot||_{1,\Omega}$ is split up into the error in Ω_c and Ω, *i.e.*, $||u-u^*||^2_{1,\Omega} = ||u-u_h||^2_{1,\Omega\setminus\Omega_c} + ||u-u_{h_c}||^2_{1,\Omega_c}$. Therefore, for $u \in H^2(\Omega)$, the quantity $||u-u^*||^2_{1,\Omega}$ is bounded by $c\max(h,h_c)|u|_{2,\Omega}$.

4 Algebraic system and implementation details

Let us now consider the algebraic form of the discrete coupled problem. Nodes in $\mathcal{T}_{h_c}$ are decomposed into a block (I) of inner and a block (Γ) of boundary nodes. The matrix K_{h_c} associated with the problem on $X_{0,h_c}(\Omega_c)$ reads

$$K_{h_c} = \begin{pmatrix} K_{II} & K_{I\Gamma} \\ 0 & \mathrm{Id} \end{pmatrix}.$$

Let us denote by Q the matrix associated to the projection operator Π, then the coupled algebraic system at each time step reads

$$\begin{pmatrix} K_h & 0 & 0 \\ 0 & K_{II} & K_{I\Gamma} \\ -Q & 0 & \mathrm{Id} \end{pmatrix} \begin{pmatrix} \mathbf{u}_h \\ (\mathbf{u}_{h_c})_I \\ (\mathbf{u}_{h_c})_\Gamma \end{pmatrix} = \begin{pmatrix} \mathbf{f}_h \\ (\mathbf{f}_{h_c})_I \\ \mathbf{0} \end{pmatrix},$$

where K_h is the global stiffness matrix associated with the Dirichlet problem on $X_{0,h}(\Omega)$. At each time step $t_{n+1} = t_n + \delta t$, for the magnetic part, we solve the above system in successive steps,

$$\mathbf{u}_h^{n+1} = K_h^{-1}\mathbf{f}_h^{n+1}, \qquad (\mathbf{u}_{h_c}^{n+1})_I = K_{II}^{-1}((\mathbf{f}_{h_c}^{n+1})_I - K_{I\Gamma}Q\mathbf{u}_h^{n+1}). \tag{9}$$

The mechanical behavior of the conducting plate is obtained by using an explicit Euler method for the velocity and an implicit Euler method for the levitation height.

As the levitation problem demands a large number of time steps, the solution of (9) goes through a LU factorization for K_h and for K_{II}, since the two matrices K_h and K_{h_c} do not change if the position of the subdomain Ω_c changes inside the global domain Ω. In fact, the physical parameters σ, ν do not depend on time and the motion is that of a rigid body. Moreover, no remeshing is necessary since we can work with overlapping meshes, but the matrix Q which represents the projection operator Π has to be reassembled whenever the subdomain Ω_c changes position, as in the considered problem. An adequate choice of Π is not only important theoretically (for optimality) but also numerically (Q easy to assemble and not increasing the computational complexity of the approach). We then adopt for Π the mortar L^2-projection operator

$$\Pi : H^1(\Omega) \to W_{h_c}(\Gamma), \qquad \int_\Gamma (\Pi v) w = \int_\Gamma v\, w, \qquad \forall w \in M_{h_c}(\Gamma), \tag{10}$$

where $M_{h_c}(\Gamma)$ is a Lagrange multiplier space. The choice of $M_{h_c}(\Gamma)$ is of key importance to have a well-defined projection operator Π which fulfills the theoretical requirements of stability and optimality. Since Γ is a closed surface, we can take $M_{h_c}(\Gamma) = W_{h_c}(\Gamma)$, [3].

We now turn to the most delicate step of the coupling between u_h defined in Ω and u_{h_c} in Ω_c, namely the definition of the values of $u_h \in X_{0,h}(\Omega)$ at the nodes of $\mathcal{T}_{h_c}$ lying on Γ. For this purpose we use the mortar projection operator defined in (10). The value $u^- = \Pi u_h \in W_{h_c}(\Gamma)$ is called non-mortar (slave) value of the mortar (master) value $u^+ = u_{h|\Gamma}$. Starting from $u_h \in X_{0,h}(\Omega)$ we have to compute Πu_h by using the coupling condition (10), *i.e.*, $\int_\Gamma (u^- - u^+)w^- = 0$ for all $w^- \in M_{h_c}(\Gamma)$. Let $\mathcal{I}_{h_c}^-$ denote the set of all nodes of the non-mortar mesh $\mathcal{T}_{h_c}$ lying on Γ, $\mathcal{E}_{h_c}$ the set of all boundary edges (faces in 3D) of $\mathcal{T}_{h_c}$ and $\mathcal{I}_h^+$ the set of all nodes of the mortar mesh $\mathcal{T}_h$ belonging to a triangle (tetrahedron in 3D) that intersects an edge (a face in 3D) of $\mathcal{E}_{h_c}$.

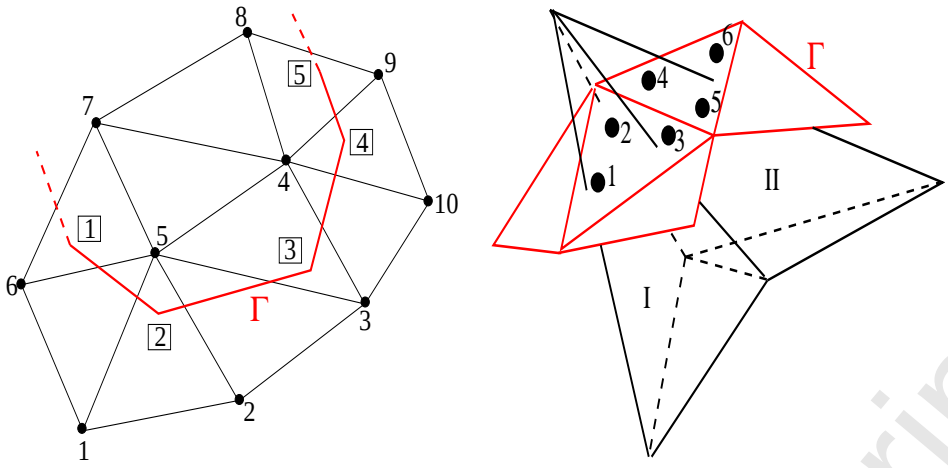

Fig. 3. Overlapping meshes in 2D and 3D, a zoom close to the interface Γ. Due to the position of segment $\boxed{2}\boxed{3} \in \Gamma$, the entries $(Q^+)_{\ell k}$ are a priori non zero for $\ell = \boxed{2}, \boxed{3}$ and $k = 1,2,3,4,5$ whereas the entry $(Q^+)_{\ell 6}$ for $\ell = \boxed{3}$ and $(Q^+)_{\ell 10}$ for $\ell = \boxed{2}$ are zero (left). The quadrature points $1,2$ fall in tetrahedron I, $3,4,5$ are in II and 6 is neither in I nor in II (right).

According to Fig. 3 left, we have

$$\mathcal{I}^-_{h_c} = \{\boxed{1}, \boxed{2}, \boxed{3}, \boxed{4}, \boxed{5}, \ldots\},$$
$$\mathcal{E}_{h_c} = \{\boxed{1}\boxed{2}, \boxed{2}\boxed{3}, \boxed{3}\boxed{4}, \boxed{4}\boxed{5}, \ldots\},$$
$$\mathcal{I}^+_h = \{1,2,3,4,5,6,7,8,9,10,\ldots\}.$$

The left-hand side of (10) is equivalent to a squared mass matrix Q^- whose entries are $Q^-_{\ell k} = \int_\Gamma \psi^-_k \varphi^-_\ell$, where ψ^-_k and φ^-_ℓ are basis functions of $W_{h_c}(\Gamma)$ and $M_{h_c}(\Gamma)$ respectively. Matrix Q^- can be easily computed since both basis functions are defined with respect to the same mesh, that of Ω_c. On the contrary, the entries $Q^+_{\ell k} = \int_\Gamma \psi^+_k \varphi^-_\ell$ of the rectangular matrix Q^+ involve discrete functions living on different meshes, as ψ^+_k is a basis function of $X_{0,h}(\Omega)$ and φ^-_ℓ of $M_{h_c}(\Gamma)$ respectively. To compute $Q^+_{\ell k}$ we have to intersect the d-dimensional support of ψ^+_k on Ω with the $(d-1)$-dimensional support of φ^-_ℓ on Γ. The exact computation of this intersection is an expensive and difficult task. The use of quadrature formulas to evaluate $Q^+_{\ell k}$ improves the implementation efficiency and can be easily done as follows:

(i) we define a quadrature formula $(y^j_i, \xi^j_i)_{j=1,\ldots N_q}$ on the face $s_i \in \mathcal{E}_{h_c}$ by mapping a chosen quadrature formula defined on a reference face;
(ii) we localize each quadrature node y^j_i within $\mathcal{T}_h$ (see for example Fig. 3 right);
(iii) we replace $Q^+_{\ell k}$ by $\sum_{s_i \in \mathrm{supp}(\varphi^-_\ell)} \sum_{j=1}^{N_q} \xi^j_i \psi^+_k(y^j_i)\varphi^-_\ell(y^j_i)$, where ψ^+_k are the

basis functions associated to the vertices of tetrahedra containing the quadrature nodes as determined in (ii)

The condition (10) in matrix form reads $Q^- v^- = Q^+ v^+$, where the two matrices Q^+ and Q^- are locally assembled, and yields $v^- = (Q^-)^{-1} Q^+ v^+$, justifying the nomenclature of slave function for v^- and master function for v^+. Matrix Q is then given by $(Q^-)^{-1} Q^+$.

A simple scheme, to which we refer as explicit coupling procedure, to solve the considered coupled electromagnetic and motion problem is the following.

- Solve the electromagnetic problem (9) at the time $t_n = n\delta t$ for a given position.
- Compute the external force acting on the conducting plate for this state.
- Assuming that the magnetic force remains unchanged over the time step, solve the equation of motion (4) to determine the displacements of the moving parts.
- Modify the position of the moving part mesh using the calculated displacements.
- Go to the next time step t_{n+1}.

5 Numerical results

We consider two numerical tests illustrating the performances of the proposed approach.

A numerical test on the method accuracy

We start by dealing with a simple problem to state the accuracy of the method. The considered model problem is $-\Delta u + u = f$ on $\Omega = [0,1]^2$ with source term f and boundary conditions consistent with the exact solution $u(x,y) = cos(2\,\pi\,x)\,y\,(1-y)$. As Ω_c we take a square patch $[0.375, 0.75]^2$ clockwise rotated of 31° around the point $(0.5625, 0.5625)$ (see Fig. 2 left). The finite element solution is visualized in the left picture of Fig. 4. The errors in the L^2- and H^1-norms are presented in Tables 1 and 2 respectively and visualized in a log-log scale in the right picture of Fig. 4. The global error $u - u^*$ decreases in the expected way, confirming the theoretical bound.

A levitation problem

We now go to the coupled magneto-mechanical problem, presenting very preliminary results. The computational domain is presented in Fig. 1 right.

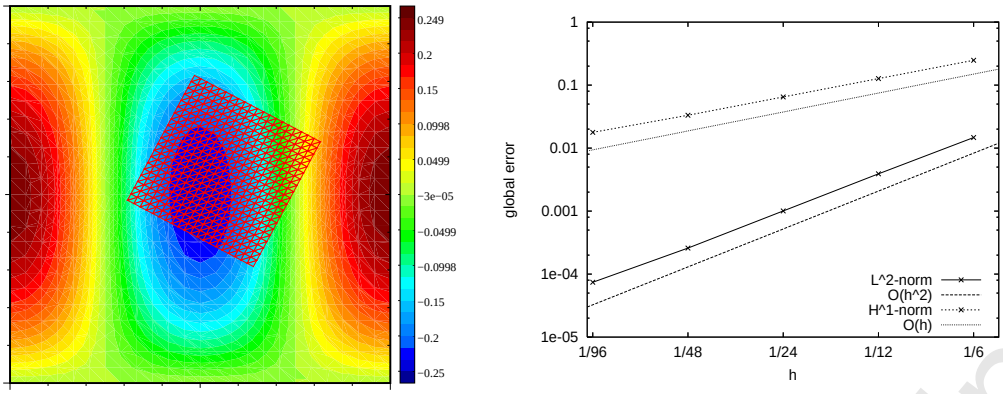

Fig. 4. The finite element solution u^* corresponding to $h = 1/24$, $h_c = 0.375/20$, and error decay in the L^2- and H^1-norms.

$\max(h, h_c)$	$\|\|e_h\|\|_{0,\Omega}$	$\|\|e_{h_c}\|\|_{0,\Omega_c}$	$\|\|u - u^*\|\|_{0,\Omega}$
1/6	$1.35\,10^{-2}$	$5.63\,10^{-3}$	$1.47\,10^{-2}$
1/12	$3.61\,10^{-3}$	$1.45\,10^{-3}$	$3.90\,10^{-3}$
1/24	$9.20\,10^{-4}$	$4.02\,10^{-4}$	$1.00\,10^{-3}$
1/48	$2.31\,10^{-4}$	$1.32\,10^{-4}$	$2.66\,10^{-4}$
1/96	$6.89\,10^{-5}$	$4.56\,10^{-5}$	$8.27\,10^{-5}$

Table 1
The L^2-norm with mortar projection.

$\max(h, h_c)$	$\|\|e_h\|\|_{0,\Omega}$	$\|\|e_{h_c}\|\|_{0,\Omega_c}$	$\|\|u - u^*\|\|_{0,\Omega}$
1/6	0.24	$5.43\,10^{-2}$	0.24
1/12	0.12	$2.57\,10^{-2}$	0.12
1/24	$6.25\,10^{-2}$	$1.70\,10^{-2}$	$6.48\,10^{-2}$
1/48	$3.13\,10^{-2}$	$1.34\,10^{-2}$	$3.40\,10^{-2}$
1/96	$1.56\,10^{-2}$	$1.11\,10^{-2}$	$1.92\,10^{-2}$

Table 2
The H^1-norm with mortar projection.

A cylindrical alluminium plate ($\sigma = 3.40\,10^7$ S/m, $m = 0.107$ Kg) is located above two cylindrical coils. All three parts are aligned coaxially. The dimensions of the device are shown in Fig. 5. The levitation height z refers to the distance between the lower edge of the plate and the upper edge of the current carrying area ($z = 0$). For $t \leq 0$, the plate rests above the coils at a distance of $z = 3.8$ mm, due to the thickness of the winding form. Both coils are connected in series, but with different sense of winding. For $t \geq 0$, sinusoidal currents $I(t) = I\sin(2\pi f t)$, $I = 20$ A and $f = 50$ Hz, flow without electrical transient in the coils in opposite direction. Due to the induced currents a repulsive force is exerted on the plate. After some damped oscillations, the plate reaches a

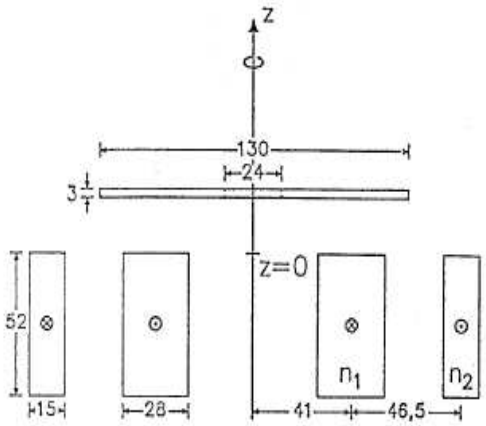

Fig. 5. Device for electrodynamic levitation as presented in [11].

stationary levitation measured position of $z = 11.3$ mm. The source current density in the coils is given by $\mathcal{J}_s(t) = \pm\frac{N}{S}I(t)$, where $N = 960$ for the inner coil, $N = 576$ for the outer coil, S is the surface of the coil (r, z)-section with a $\pm$ sign depending on the flow direction. For the spatial discretization, we use linear finite elements, the mesh in Ω (resp. in Ω_c) is composed of $50 \times 50 \times 2$ (resp. $50 \times 20 \times 2$) triangles. The two meshes overlap without matching neither on Γ nor in Ω_c. A characteristic dimension of the problem is the depth of penetration of the magnetic field in the domain Ω_c, given by

$$\delta = \frac{1}{\sqrt{\pi\,\mu_0\,\sigma\,f}}.$$

With the given data, we have $\delta \approx 0.01$ that means four times the plate thickness. The source field flux lines cross the plate and so the induced field in the conductor is not zero but its action on the source field is neglected.

In the left picture of Fig. 6, we present the source field generated by the coils (dark colors refer to negative values and light color to positive ones). In the right picture of Fig. 6, we show the computed levitation height as a function of time. We have performed 2000 steps with $\delta t = 100\,10^{-6}$s. The period of oscillation agrees with the measured one, whereas some discrepancies appear in the oscillation amplitude.

The velocity as well as the total external force are shown in Fig. 7 as functions of the levitation height. At the beginning the plate passes through the equilibrium position with too much kinetic energy stored and cannot stabilize instantaneously. Thus, it slows down but doesn't stop. We can observe the same phenomenon each time the force and the weight are equal. On Fig. 7 right we can observe a sort of hysteresis cycles around the equilibrium position. Without this phenomenon, the plate would never stop in the considered time interval (it would stop in a larger time interval due to the air resistance).

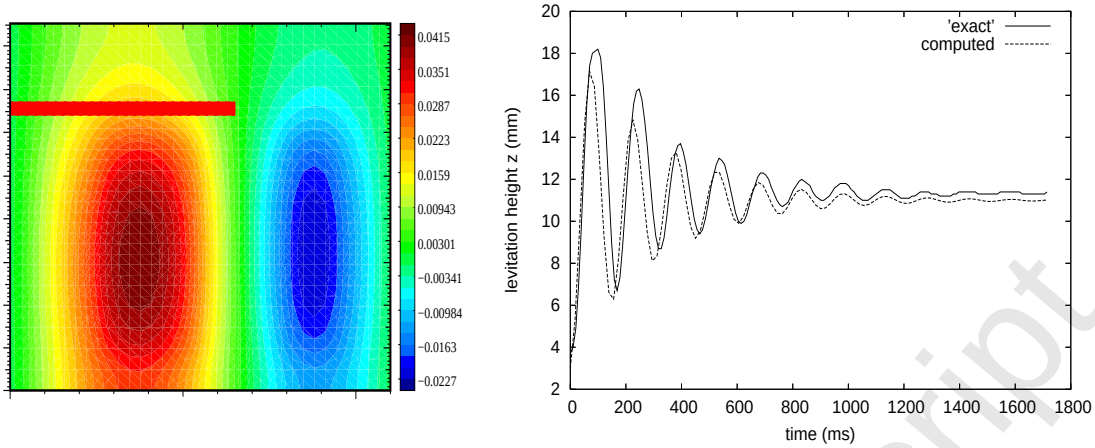

Fig. 6. The magnetic vector potential component $\mathcal{A}$ associated to the source field after some time steps (left) and measured versus computed levitation height (right).

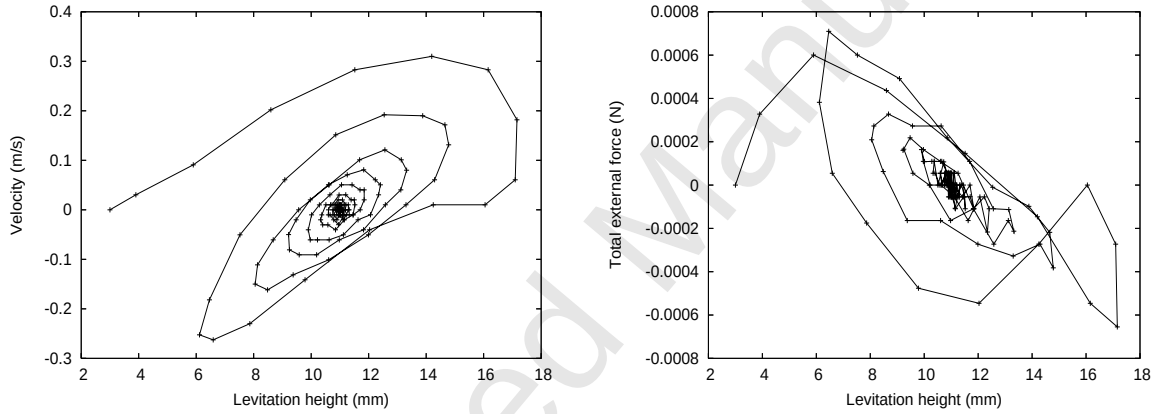

Fig. 7. Computed external total force (left) and velocity (right) visualized with respect to the levitation height.

The surface of the cycles corresponds to losses related principally to the Joule effect in the conductor and a potential energy variation as soon as the plate changes height. The dissipation of these energies contributes to the system stabilization. A deeper analysis of the energy assessment has to be performed as the force cycles are difficult to see.

References

[1] Y. Achdou, Y. Maday, The mortar element method with overlapping subdomains, SIAM J. Numer. Anal. 40 (2002) 601-628.

[2] R. Albanese, G. Rubinacci, Formulation of the eddy-current problem, IEE Proc. A 137 (1990) 16-22.

[3] C. Bernardi, Y. Maday, A. Patera, A new nonconforming approach to domain decomposition: the mortar element method, in Nonlinear Partial Differential Equations and Their Applications, H. Brezis and J.L. Lions, eds. Pitman (1994) 13-51.

[4] A. Bossavit, Computational Electromagnetism, Academic Press, Springer (1998).

[5] F. Brezzi, J.-L. Lions, O. Pironneau, Analysis of a chimera method, C. R. Acad. Sci. Paris, Ser. I. 332 (2001) 655-660.

[6] X.-C. Cai, M. Dryja, M. Sarkis, Overlapping nonmatching grid mortar element methods for elliptic problems, SIAM J. Numer. Anal. 36 (1999) 581-606.

[7] B. Flemisch, Y. Maday, F. Rapetti, B. I. Wohlmuth, Scalar and vector potentials' coupling on nonmatching grids for the simulation of an electromagnetic brake, Int. J. for Comp. and Math. in Electric and Electronic Eng. 24 (2005) 1061-1070.

[8] B. Flemisch, B. I. Wohlmuth, A domain decomposition method on nested domains and nonmatching grids, Numer. Methods Partial Differ. Equations 20 (2004) 374-387.

[9] R. Glowinski, T. W. Pan, J. Periaux, A fictitious domain method for Dirichlet problem and applications, Comp. Meth. in Appl. Mech. and Engng. 3 (1994) 283-304.

[10] R. Glowinski, J. He, J. Rappaz, J. Wagner, Approximation of multi-scale elliptic problems using patches of finite elements, C. R. Acad. Sci. Paris, Ser. I 337 (2003) 679-684.

[11] H. Karl, J. Fetzer, S. Kurz, G. Lehner, W. M. Rucker, Description of TEAM Workshop Problem 28: An Electrodynamic Levitation Device (1996) http://www.compumag.co.uk/problems/problem28.pdf.

[12] S. Kurz, J. Fetzer, G. Lehner, Three-dimensional transient BEM-FEM coupled analysis of electrodynamic levitation problems, IEEE Trans. on Magn. 32 (1996) 1062-1065.